

# COMPOSITION AND DIAGENETIC PROCESSES OF SANDSTONE AND TUFF DEPOSITS OF THE CENOMANIAN CARDIEL FORMATION, CARDIEL LAKE AREA, PROVINCE OF SANTA CRUZ

Renato R. Andreis<sup>1</sup>, Patricia E. Zalba<sup>2</sup> and M. E. Morosi<sup>2</sup>

<sup>1</sup> Museo Paleontológico Egidio Feruglio, Av. Fontana 140, 9100 Trelew, Chubut. E-mail: rrandreis22@hotmail.com

<sup>2</sup> Centro de Tecnología de Recursos Minerales y Cerámica (Cetmic), Comisión de Investigaciones Científicas de la Provincia de Buenos Aires. Facultad de Ciencias Naturales y Museo de La Plata. E-mail: pezalba@netverk.com.ar

**RESUMEN:** *Composición y procesos diagenéticos de los depósitos de arenisca y toba de la Formación Cardiel (Cenomaniano), área Lago Cardiel, provincia de Santa Cruz.*

La Formación Cardiel de alrededor de 200 m de espesor en el área estudiada, contiene diferentes tipos de depósitos volcanoclásticos, mayormente representados por tobas finas y bentonitas, y epiclásticos subordinados como areniscas líticas con colores castaño amarillentos, amarillentos u oliva claros, limolitas y arcilitas. Paleosuelos de tonalidad rojiza con algunas raíces axiales y débiles estructuras prismáticas aparecen en el tope de las limolitas, tobas o bentonitas. Las tufitas y tobas contienen los mismos componentes neovolcánicos, junto a abundantes vitroclastos y menor cantidad de fragmentos pumíceos. Diferentes tipos de vitroclastos pueden ser reconocidos dentro de esta unidad, mientras que los fragmentos pumíceos están representados por diversas variedades vesiculares. Clastos de tobas son frecuentes en las tufitas. Casi todas las muestras contienen montmorillonita diagenética y pedogenéticamente infiltrada, como así también zeolitas. Fueron identificadas clinoptilolita Ca-Na-K (Si/Al>4) predominante, y menor cantidad de analcima (Si/Al cerca de 3). La esmectita y la clinoptilolita pueden reemplazar los vitroclastos y los fragmentos pumíceos, o rellenar espacios, mientras que la esmectita también forma finos cutanes. La secuencia de procesos diagenéticos incluye la transformación (hidrólisis) del vidrio a esmectita, y luego a zeolitas. Además, las zeolitas preceden el crecimiento de calcita (a veces reemplazan vitroclastos o fragmentos pumíceos), y la infiltración de óxidos-hidróxidos de hierro. La variación vertical de las zeolitas puede ser explicada por la existencia de aguas percolantes en un sistema hidrológico abierto. La presencia de zeolitas a lo largo de todo el perfil analizado permite asignar esta asociación mineralógica a la zona de clinoptilolita. La interpretación paleoambiental de la Formación Cardiel incluye la presencia de corrientes mareales en amplias albuferas. Las paleocorrientes medidas en las areniscas revelan direcciones dominantes de transporte de sedimentos hacia el norte, noreste, y en menor medida, hacia el sudoeste. El paulatino incremento en el contenido de tobas y bentonitas cubriendo las albuferas y formando amplias planicies favoreció el desarrollo de paleosuelos. La abundancia de vitroclastos indica un origen magmático desde los volcanes situados a lo largo de la Cordillera de los Andes. Probablemente ocurrieron procesos alternantes de volcanismo pliniano y sub-pliniano y, tal vez, breves procesos de volcanismo freato-pliniano.

Palabras clave: *Formación Cardiel, volcanoclásticos, zeolitas, pedogénesis, diagénesis.*

## ABSTRACT:

The Cardiel Formation (Cenomanian), around 200 m in thickness in the studied area, includes different types of volcanoclastic deposits, mainly represented by fine tuffs and massive bentonites, and subordinated epiclastics such as lithic sandstones of yellowish-brown, dusky yellow, or light olive hues, siltstones and claystones. Reddened paleosols with some small axial roots and weak prismatic structures appear on top of siltstones, tuffs and bentonites. Tuffites and tuffs contain the same neovolcanic components, abundant glass shards and minor pumices. Different types of glass shards can be differentiated within this unit, whereas pumice fragments are represented by different vesicular varieties. Vitreous tuffaceous clasts are abundant in the tuffites. Almost all samples contain not only diagenetically-derived, but also pedogenetically-infiltrated montmorillonite, as well as zeolites. Predominant Ca-Na-K clinoptilolite (Si/Al>4) and minor analcime (Si/Al near 3) were identified. Smectite and clinoptilolite may either replace glass-shards or pumices, or fill pore spaces, whereas smectite also appears as thin cutans. The sequence of diagenetic processes includes the conversion (hydrolysis) of glass to smectite, and later to zeolites. Furthermore, zeolites preceded calcite growth (sometimes replacing glass-shards or pumices), which in turn, formed prior to pervading ferric oxides-hydroxides. The vertical distribution of zeolites can be explained taking into account the presence of percolating waters in an open hydrologic system. The zeolite content throughout the whole profile links the mineralogical association observed within the sediments of the Cardiel Formation to the clinoptilolite zone. Paleoenvironmental reconstructions for the Cardiel Formation point out to tidal currents taking place in wide lagoons; tuffaceous and bentonitic deposits covered those ancient lagoons forming wide, flat plains on which paleosols developed. Paleocurrents measured on sandstone beds indicate main sediment transport directions towards the north, northeast, and less frequently to the southwest. The abundance of glass shards thorough this unit indicates a magmatic origin related to the volcanoes situated along the Andean Mountains possibly associated with alternating plinian and subplinian eruptions with brief phreato-plinian processes.

Keywords: *Cardiel Formation, volcanoclastics, zeolites, pedogenesis, diagenesis.*

## INTRODUCTION

The Cardiel Formation crops out at the northern, western and southern part of the Cardiel Lake (Figs. 1a y b), where its stratotype was defined (Russo and Flores 1972; Russo *et al.* 1978). Previous research was carried out by Piatnitsky (1938) and Ugarte (1956), and years later, Ramos (1982) and Arbe (1989) offered new geological information. The basal part of the unit (around 80 m in thickness) is composed of gray, green, rose, and yellow shales, and yellow to greenish white tuffs, whereas its middle part (around 70 m in thickness) includes poorly stratified reddish mudstones and white tuffs (Ramos 1982). The Cardiel Formation lies conformably on the underlying Piedra Clavada Formation, characterized by marine and littoral sequences containing gray and yellowish partially silicified tuffs in its upper part (Fossa Mancini *et al.* 1938). The Cardiel Formation is about 270 m in thickness and is considered Cenomanian in age due to the presence of rare *Classopolis torosus* (Pothe de Baldis 1978), as well as some dinosaur remains identified at the Tunas peninsula and near the Las Tunas farm (Piatnitsky 1938). The middle part of the unit also contains silicified trunks. To the west of the Cardiel Lake, Ruiz (1984) found remains of gymnosperm seeds identified as *Carpolithus* sp.

The goal of this paper is to analyze the post-depositional processes that affected the volcanoclastic sediments of the Cardiel Formation, taking into account their depositional environment and hydrologic regime. Thus, main focus has been put to the zeolite and clay minerals origin and diagenetic transformations, petrology of epi- and pyroclastic parental material (i.e., sandstones, tuffs and tuffites) and related pedogenetic processes.

## GEOLOGICAL SETTING

Several stratigraphical and sedimentological observations on the Cardiel Formation were made in the surroundings of the north-northeastern border of the Cardiel Lake, near Cerro Crater Apagado (Fig. 1b). A measured stratigraphic section of 196 m in thickness (Fig. 2) includes several types of

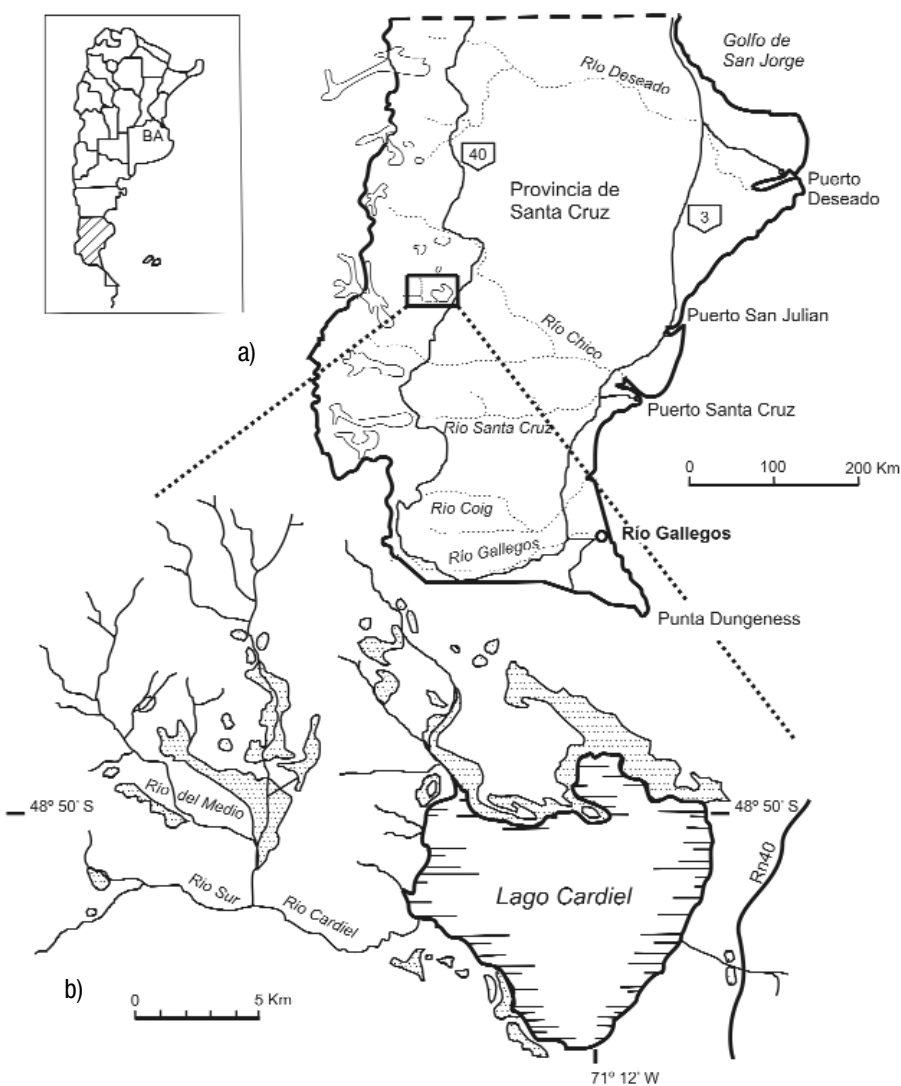


**Figure 1:** a) Location of the Cardiel Lake in the province of Santa Cruz. b) Enlarged view of the Cardiel Lake area in A) showing the outcrops of the Cardiel Formation (dotted areas) and the localities studied in this work: 1. Cerro Crater Apagado; 2. Ea. Las Tunas; 3. Ea. Cerro Bayo; 4. Cerro Mesa; 5. Ea. La Angelina; 6. Ea. Río del Medio; 7. Ea. La Cabaña; 8. Ea. Rincón de los Toros; 9. Cerro Pelado; 10. Cerro Karken o Cóndor; 11. Ea. Dos Hermanos; 12. Police; 13. Ea. La Siberia.

volcanoclastic sediments (79%), as well as claystones and siltstones (21%); volcanoclastic sediments are represented by tuffaceous rocks (51%), bentonites (24%), and lithic sandstones (4%).

Volcanoclastic sandstone deposits consist of massive to poorly laminated beds with some ripple marks or small trough crossbedding structures. Clay-rich intraclasts and scarce quartz clasts (1-2 cm diameter) can be observed within the beds. These rocks are light yellow or yellowish-brown, and appear as lenticular and tabular beds of metric thickness. Tuffs show horizontal bedding,

and their relatively good sorting is attributed to the grain size fractionation during eolian transport. Tephra-sized deposits are the most represented (83%), but some medium sand size (11%) or silty varieties (6%) are also present. Their colors are light yellowish-brown, yellow or white, and less frequently gray, greenish-gray, rose-gray, yellowish-gray, or olive hues. Some lenses rich in pumice fragments from 1 to 5 cm in diameter were found. Tuffs (e.g. Fig. 2, sample 14) also contain scarce globulolite type microphytoliths. Bentonites are massive and olive, dark olive or yellowish-brown in color.

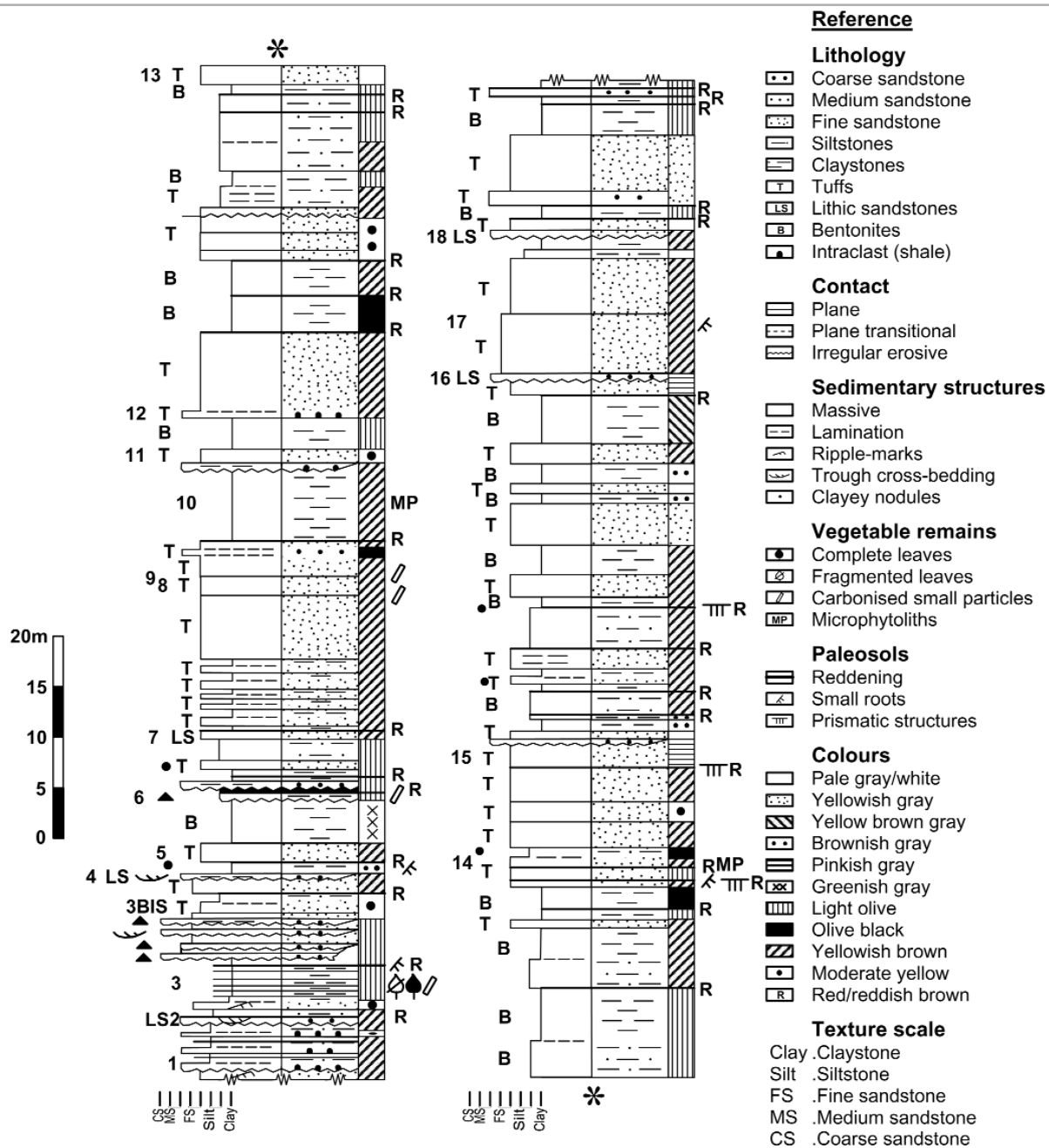


Figure 2: Schematic log of the Cardiel Formation near Cerro Cráter Apagado. See legend for references.

Fine-grained clastic sediments consist of yellowish-green, olive, and yellowish-brown massive claystones, as well as clayey to sandy massive or poorly laminated siltstones. Also, some olive-gray or dark olive colors are distinguishable. Some microphytoliths of the globulolite type, characteristic of palm trees, have been found in the claystones. Carbonized vegetal remains are also frequent at the base of the section (Fig. 2). Paleosols are very frequent in the studied

unit, represented by the reddening on the top of siltstones, tuffs or bentonite deposits. In the case of siltstones and tuffs, some small axial roots and poorly developed prismatic structure were recognized (Fig. 2). Paleocurrents measured on directional structures within the volcanoclastic sandstone beds revealed that dominant currents flowed to the north and northeast; rare currents were oriented to the southwest.

## MATERIALS AND METHODS

Thirteen samples (7 tuffs, 5 tuffites and 1 lithic sandstone) were analyzed by optical microscopy and X-ray diffraction. Scanning electron microscopy (SEM), EDAX, atomic absorption chemical analyses and X-ray diffraction quantitative analyses were carried out on selected tuff samples. A petrographical optical microscopy Olympus BX60 was used for thin section observations. X-

ray diffractometry was performed using Philips 3020 equipment, applying Cu K $\alpha$  radiation (40 kV and 20mA) and Ni filter. Step scan data were collected from 3 to 70° 2 $\theta$  with a step of 0.02° and a counting time of 2 sec/step. The divergence, receiving and scattering slits were 1°, 0.2° and 1° respectively; no monochromator was used. Routine determinations were carried out on the <2 $\mu$  size fraction in natural, glycolated (overnight) and heated (500°C for 2 hrs.) samples. Greene-Kelley test (Greene-Kelley 1953) was carried out to identify the smectite type. A Phillips 505 scanning electron microscopy and EDAX were used for zeolite identification. Total samples (chips) were analyzed under SEM. Quantitative analysis was carried out applying the Rietveld method (Rodríguez-Carvajal 1990) to selected tuff sample X-ray patterns using the FULLPROF program (Young 1993).

## QUANTITATIVE ANALYSIS USING THE RIETVELD METHOD

Quantitative results obtained using the Rietveld method on selected tuff samples are shown in Table 1. The content of non-crystalline phases was analyzed adding a known amount of micronized fluorite as internal standard. Bulk chemical analyses used in the calculations are shown in Table 2. The analysis of the samples with fluorite addition by the Rietveld method revealed that the content of non-crystalline or not-detected phases by X-ray diffraction is always less than 5 % in weight. Chemical analyses and loss on ignition are compatible with the given results; however, sample 3 may actually contain more calcite than the calculated amount due to the fact that loss on ignition and Ca content for this sample are larger than the amounts obtained by the above mentioned method.

## CLASSIFICATION AND DESCRIPTION OF THE SEDIMENTS

Following the classification schemes of Terruggi *et al.* (1978), Mazzoni (1986) and Pettijohn *et al.* (1987), pyroclastic sediments of the Cardiel Formation represented by fine-

**TABLE 1:** Composition of selected tuff samples (in weight %) applying the Rietveld method

Sample	Quartz (%)	Clinoptilolite (%)	Montmorillonite (%)	Sanidine (%)	Oligoclase (%)	Calcite (%)
3	38	21	14	17	9	<1
12	28	30	27	10	4	n.d.
14	38	2	30	22	7	n.d.

References: n.d., not detected

**TABLE 2:** Bulk chemical analyses of selected tuff samples

Sample	SiO <sub>2</sub> (%)	Al <sub>2</sub> O <sub>3</sub> (%)	Fe <sub>2</sub> O <sub>3</sub> (%)	MgO (%)	CaO (%)	Na <sub>2</sub> O (%)	K <sub>2</sub> O (%)	TiO <sub>2</sub> (%)	P <sub>2</sub> O <sub>3</sub> (%)	MnO (%)
3	68,89	10,85	1,65	0,36	3,73	0,92	3,93	0,25	0,02	0,35
12	66,69	12,65	2,55	0,70	1,62	2,02	2,03	0,27	0,04	0,09
14	67,89	13,99	1,85	0,55	1,92	1,14	3,98	0,31	0,02	0,07

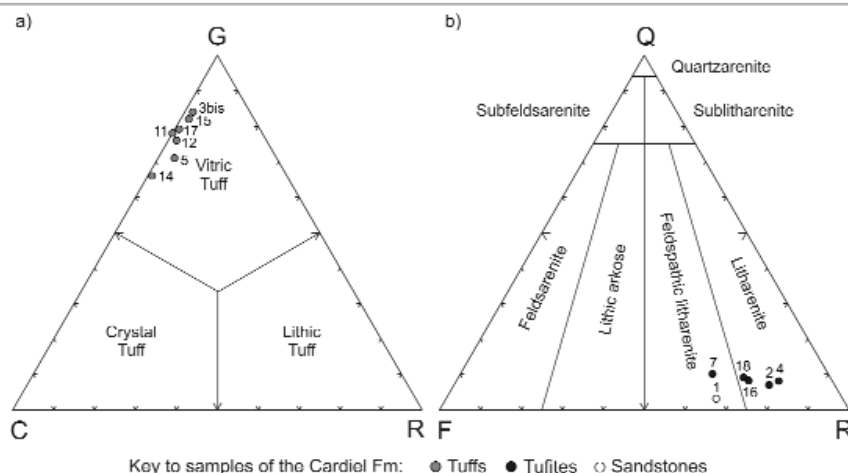


**Figure 3:** a) GCR (glass-crystals-rock fragments) diagram showing tuff samples composition (grey dots); classification fields as in Pettijohn *et al.* (1987). b) QFL (quartz-feldspars-rock fragments) diagram showing sandstone and tuffite samples of the Cardiel Formation (white and black dots, respectively); classification fields after Folk *et al.* (1970). All data extracted from recalculated parameters shown in Table 3.

to medium-grained tuffs can be classified as vitric tuffs (samples 3bis, 5, 11, 12, 14, 15, 17; Fig. 3a). Associated epiclastic sediments such as volcanoclastic sandstones are characterized by having their pyroclastic clasts reworked by tractional water currents in shallow channels; they can be classified using the schema of Folk *et al.* (1970) (Fig. 3b) either as lithic tuffites (tufo-rudites and tufo-arenites; samples 2, 4, 16, 18) or feldspathic lithic tuffites (sample 7), whereas some subordinated feldspathic litharenites are also present (sample 1).

The presence in these rocks of abundant monocrySTALLINE quartz and sanidine, but scarce plagioclase, suggests that the original magma must have been of rhyolitic composition.

Both tuff (pyroclastic) and tuffite (epiclastic)

deposits contain the same neovolcanic components (i.e., crystalline, lithic and vitric fragments) (Fig. 4), thus, an integrated description of these components is given in the following paragraphs. Tuffites show a low degree of compaction, revealed by their clasts having tangential contacts.

## CRYSTALLINE COMPONENTS

Crystalline components include broken, euhedral monocrySTALLINE quartz without inclusions, and a few grains of polycrySTALLINE quartz probably related to the infill of vesicles (i.e., amygdals). Feldspars are represented by broken euhedral clean crystal of sanidine, some with Carlsbad twins, and clean plagioclase of oligoclase composition (An 20-26%), with Albite, Carlsbad-Albite

and minor Carlsbad twins, showing glass inclusions. Plagioclase crystals may have no zonal structures, or show less normal or recurrent zonation. Altered brown biotite was also recognized. In few tuffites some grains of magnetite, apatite and zircon were identified (Table 3).

### LITHIC COMPONENTS

Lithic components comprise volcanic fragments, and lithic tuff clasts (Table 3). These lithic fragments exhibit a variable degree of roundness, being typically angular in tuffaceous sediments, but showing some roundness in the volcanoclastic sandstones. Lithic fragments of volcanic origin include trachytic, rhyolitic and less common andesitic grains, with different textures such as hialopilitic, radial fibrous, pilotaxitic, trachitic, intersertal, and felsitic. Many clasts show the complete replacement of the original glass by limonite or hematite.

Tuffaceous lithic clasts are related to vitreous tuffs with planar-like, crescent and Y-shaped, massive blocky and branched shards, together with some sanidine crystals and few vesicular pumice fragments.

Very scarce ignimbrite fragments and graphic intergrowths (orthoclase-quartz), as well as wackes and siltstones clasts were identified among the components of lithic sandstones (e.g., sample 1, Table 3).

### VITRIC COMPONENTS

Vitric components comprising pumice and shards are more abundant within tuffs (average 77%) than within tuffites (average 45%) or within sandstones (36%) (Table 4 and Fig. 4). Vitric fragments are completely altered to smectite or clinoptilolite (Fig. 5). Shard clasts are very abundant in the tuffs, represented by plate-like, crescent-shaped and branched types, with minor proportion of Y-shaped and blocky (massive) individuals (Table 4). Small pumice fragments of the vesicular type are also found, represented by either small vesicle aggregates, bigger vesicles with thin walls, or slightly to highly elongated vesicles. Some altered glass clasts (obsidian) were also found. Fine-grained tephra (shards) seems to be the product of pumice comminution (cf., Heiken and

**TABLE 3:** Composition of rock samples of the Cardiel Formation

Sample	Glass (%)	VLC (%)	TLC (%)	SLC (%)	PLC (%)	Qm (%)	San (%)	Plg (%)	Biot (%)	Op (%)
<b>Sandstones</b>										
1	36	23	3	1	1	3	20	10	3	--
<b>Tuffites</b>										
2	58	4	15	--	--	7	14	2	--	--
4	58	4	16	--	--	8	11	2	1	--
7	55	3	3	--	--	10	23	5	--	1
16	24	14	32	--	--	8	16	4	1	1
18	29	12	28	--	--	9	15	6	--	1
<b>Tuffs</b>										
3bis	84	1	1	--	--	10	3	1	--	--
5	71	3	1	--	--	9	11	5	--	--
11	78	--	--	--	--	7	10	2	3	--
12	76	1	1	--	--	7	9	2	4	--
14	66	1	--	--	--	15	12	5	1	--
15	82	1	1	--	--	8	7	1	--	--
17	79	1	--	--	--	10	8	2	--	--

Key to rock components: VLC: volcanic lithic clasts; TLC: tuffaceous lithic clasts; SLC: sedimentary lithic clasts; PLC: plutonic lithic clasts; Qm: monocrystalline quartz; San: Sanidine; Plg: plagioclase; Biot: biotite; Op: opaque accessory minerals (e.g., magnetite).

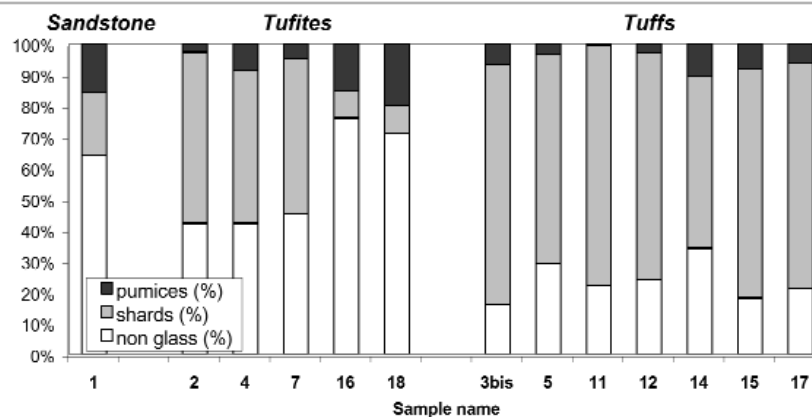


**Figure 4:** Relative content of non-glass, shards and pumice fragments in selected samples of the Cardiel Formation. Data extracted from Table 4.

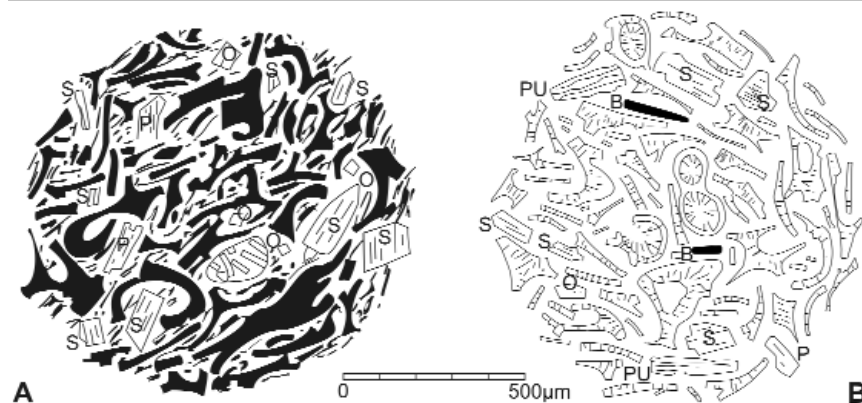


**Figure 5:** Composition of tuffs. A - Sample 11. Glass shards are substituted by hematite (black) and montmorillonite, Q: monocrystalline quartz; S: Sanidine; P: Plagioclase; V: Volcanic lithic clasts. B - Sample 12. Glass shards and pumices (PU) are substituted by reddish-stained clinoptilolite; prismatic clinoptilolite crystals precipitated within the vesicles, Q: monocrystalline quartz; S: Sanidine; P: Plagioclase; B: Biotite.

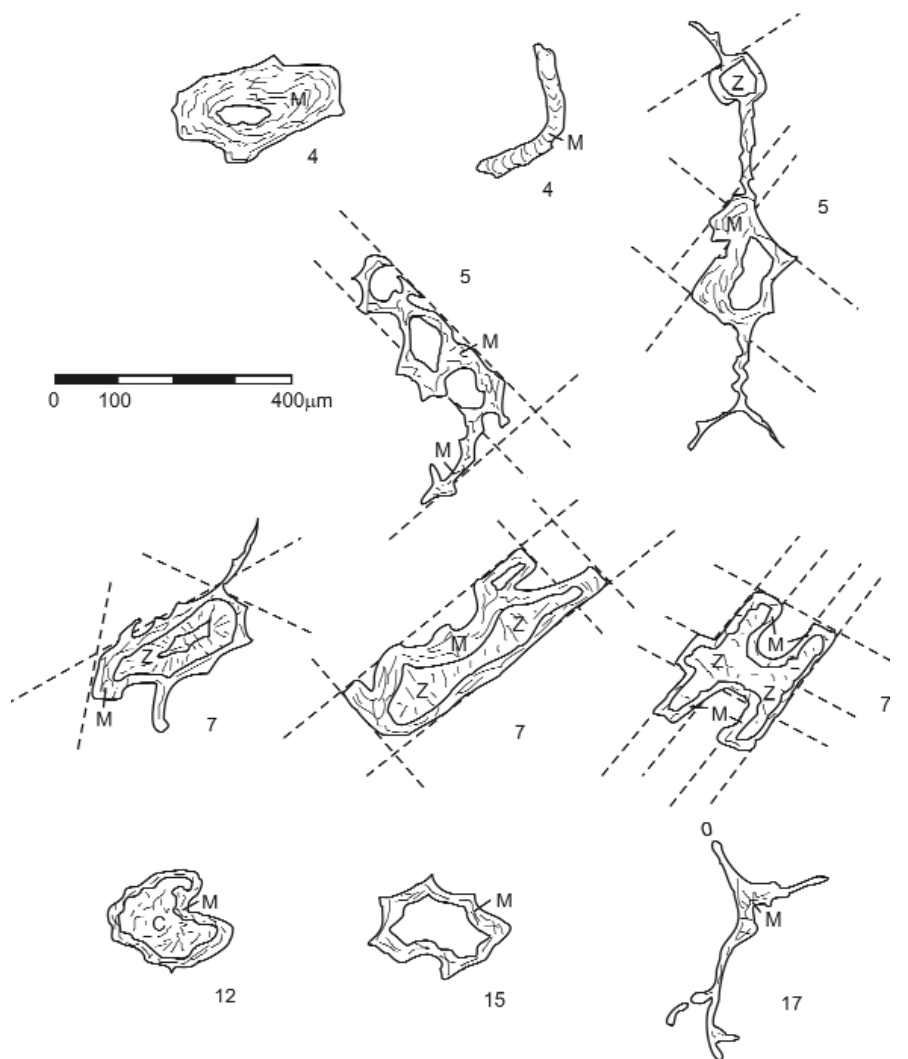


**Figure 6:** Sketches showing vugs and veins in tufites and tuffs (described from top to bottom, left to right). Sample 4: Vug filled with montmorillonite (cutan), and a curved vug made by worms, filled with montmorillonite. Sample 5: Irregular, oriented, joint-related secondary vugs filled with montmorillonite, or with montmorillonite and clinoptilolite. Sample 7: Irregular, oriented secondary vugs filled with montmorillonite (M), clinoptilolite (Z), and calcite (C); others are filled with montmorillonite (M) and clinoptilolite (Z). Sample 12: Oval-shaped vug filled with montmorillonite (M) and calcite (C). Sample 15: Oval-shaped vug filled with montmorillonite (M, vug cutan). Sample 17: Branched root filled with montmorillonite (M).

Wohletz 1992).

The same shards may appear, although in minor quantities, in the tufites (Fig. 4); Y-shaped and massive shards diminish in their proportion, whereas pumice fragments increase their frequency showing small spherical, slightly or highly elongated, and even twisted, vesicles (Table 4).

#### PEDOGENETIC PROCESSES

Pedogenetic processes were identified in the Cardiel Formation based on the recog-

nition of several key macro- and microstructures and/or textures of edafic origin. Different types of primary vugs found in tuffs and tufites are schematized in figure 6. These vugs, characterized as micro (5-30  $\mu\text{m}$ ) and mesovugs (30-75  $\mu\text{m}$ ), are associated to channels, probably attributed to the presence of worms. The vugs are partially filled by argillaceous or ferri-argillaceous cutans of montmorillonite composition, occasionally stained with hematite (Fig. 6, sample 4). Other vugs are filled with montmorillonite-calcite (Fig. 6, sample 12) or

exclusively with montmorillonite (Fig. 6, sample 15). Branched pedotubules and small veins related to root systems are filled with argillaceous cutans of smectite (Fig. 6, sample 17). In some tufites and tuffs (samples 4 and 5, respectively), papules with continuous fabric and sharp external boundaries can be identified (cf. Brewer 1964, Bullock *et al.* 1985).

Peds (Fig. 2) are weakly developed and show a prismatic structure with plane or slightly curved faces (cf. Brewer 1964, Bullock *et al.* 1985). Xenotopic and poikilotopic calcite crystals (sample 1; cf. Bullock *et al.* 1985) as well as calcitans (Brewer 1964), deposited first, are probably of phreatic origin.

Clay and zeolite assemblages and diagenetic related processes in tuffs and sandstones. Data obtained from X-ray diffraction and optical and scanning electron microscopy (Table 1) revealed that all the tuffs contain variable montmorillonite (from 12 to 35%), whereas zeolites are present in different proportions (2 to 30%) in almost all samples (only one sample is zeolite-free, sample 11). Very scarce amounts of calcite (average 1%, except sample 1 with 20% carbonate) and abundant ferric oxides-hydroxides (limonite and hematite) are present throughout the whole profile.

Many tuffs show parallel fissures but in some tufites the grains are slightly oriented. Fissures and related secondary vugs are filled with a secondary generation of montmorillonite, and later with calcite. In the tufites it is possible to see partially oriented montmorillonite lenses. The infiltration of smectite in fissures and secondary vugs may be due to the mechanical transportation of clayey material as a later migration process. Then, precipitation of large clinoptilolite crystals occurred within the remaining space of those secondary vugs. The orientation of secondary vugs is probably related to joint systems (Fig. 6, samples 5 and 7). Zeolites are represented by dominant Ca-Na-K clinoptilolite as characterized by EDAX, with Si/Al ratio  $> 4$  (Boles 1971), and very scarce analcime (Si/Al ratio near 3) as detected in the middle of the Cardiel Formation profile (samples 10 and 14, Fig. 2). Traces of a fibrous zeolite (mordenite?, erionite?) were identified in one sample

**TABLE 4:** Relative abundance of non-glassy (lithic and crystalline fragments) vs. glassy (shards and pumice fragments) components for each sample

Sample	Total Non-Glass (%) <sup>1</sup>	Total Shard (%)	Total Pumice (%)	Detail of glassy components (recalculated to 100%)										
				pSh (%)	cSh (%)	bSh (%)	ySh (%)	mSh (%)	sPu (%)	mPu (%)	oPu (%)	wPu (%)	fPu (%)	dPu (%)
<b>Sandstones</b>														
1	64	20	16	28	2	19	1	6	14	4	11	11	--	4
<b>Tuffites</b>														
2	42	55	3	60	17	10	6	2	1	--	--	2	2	--
4	42	49	9	32	42	11	--	--	--	--	--	--	15	--
7	45	50	5	55	18	10	4	4	4	--	--	1	4	--
16	76	9	15	8	5	23	--	--	10	--	19	35	--	--
18	71	9	20	11	2	15	1	2	5	--	23	30	--	11
average	55	34	10	33	17	14	4	3	5	--	21	17	7	11
<b>Tuffs</b>														
3bis	16	77	7	54	28	6	3	1	--	1	2	--	5	--
5	29	67	4	48	23	20	3	1	--	2	--	--	3	--
11	22	77	1	21	18	51	9	--	1	--	--	--	--	--
12	24	73	3	18	27	46	3	2	--	--	1	--	3	--
14	34	55	11	32	24	24	1	3	5	--	--	--	11	--
15	18	74	8	30	18	28	6	8	1	1	--	6	2	--
17	21	73	6	25	23	37	6	1	1	--	2	2	3	--
average	23	71	6	33	23	30	4	3	2	1	2	4	5	--

(1) Total percentage of non-glassy components as in Table 3. Key to rock components: pSh: planar shards; cSh: curvilinear shards; bSh: branched shards; ySh: Y-shaped shards; mSh: massive shards; sPu: small spherical vesicle pumices; mPu: moderate size vesicle with thin wall pumices; oPu: oval stretched vesicle pumices; wPu: wide elongate tubular vesicle pumices; fPu: fine elongate tubular vesicle pumices; dPu: deformed wide or fine elongate tubular vesicle pumices.

(sample 12).

Clinoptilolite crystals exhibit monoclinic habit and well developed coffin-shaped crystals under SEM and optical microscope; clinoptilolite is usually replacing planar-shaped shards and filling vugs with euhedral platy crystals several microns in length and 1-2 microns thick (Fig. 7a). Mordenite (?) was recognized under the SEM as a later phase intergrown with earlier clinoptilolite crystals (Fig. 7b). Mordenite (?) crystals are only a few tenths of a micron in length, and appear as a minor component (less than 10%). Very scarce analcime was recognized under the SEM and EDAX by its characteristic cubo-octahedral habit. Isolated subhedral analcime crystals up to 90  $\mu\text{m}$  in length were rarely seen (Fig. 7c), filling pores (sample 14) or fissures (sample 10). In tuffs samples, montmorillonite shows characteristic honeycomb texture and it is usually stained by limonite or some hematite; it occurs filling cavities (Fig. 7d) or cracks, or replacing glass shards and pumice fragments. The presence of argillaceous cutans is common in volcanoclastic sandstones and tuffs

of the Cardiel Formation. These cutans partially fill simple or branched channels, ovoid-shaped vugs or chambers, or are developed around grains. Clays constitute the first mineral group formed diagenetically from glass (Fig. 7a); the widespread presence of clays as interstitial component indicates that glass was an abundant component in the parental sediments.

In the lithic sandstones (e.g., sample 1, probably related to a phreatic level?), some glass shards and pumice fragments are completely replaced by calcite cement. This replacement process is related to the precipitation of small calcite cutans (calcitans) around the clasts, being those primary pores later filled with xenotopic and poikilotopic calcite crystals of millimetric size (cf. Brewer 1964, Bullock *et al.* 1985). In other tuffs samples (e.g., samples 3, 11, 12, 14) or tuffites (e.g., sample 7), pumice fragments are partially replaced by open calcite aggregates (Fig. 7e).

The Si/Al ratio of the analyzed clinoptilolite as revealed by EDAX is in agreement with the presence of predominant  $\text{Ca}^{++}$

over  $\text{N}^{+}$  and  $\text{K}^{+}$  as exchangeable cations, as stated by Hay (1978), being this zeolite usually rich in Ca (Irijima 1978), as in the case of the samples analyzed in this work. On the other hand, composition of the analcime is mainly controlled by the composition of the parental material, or by the chemical environment. Analcime in siliceous tuffs (or marine environment) is  $\text{SiO}_2$ -rich, generally having Si/Al ratios between 2.4 to 2.7 (Saha 1959, Wilkinson and Whetten 1964, Coombs and Whetten 1967). In the case of the samples of the Cardiel Formation, the Si/Al ratio for analcime is near 3 (samples 3 and 14). The rare occurrence of analcime is probably due to a slight change in the pH of the interacting fluids, which may have increased the  $\text{Na}^+/\text{H}^+$  ratio, and decreased the Si/Al ratio, thus favoring the crystallization of analcime (Boles 1971). Nevertheless, rare analcime of the fissure type found in one sample (sample 10) may be related to migration processes.

## SEQUENCE OF CRYSTALLIZATION

Experimental studies carried out by Höller and Wirsching (1978) using rhyolitic glass as a starting parental material helped to establish the sequence of diagenetic events that affected the sediments of the Cardiel Formation, making clear the processes involved in the alteration of volcanic and volcanoclastic material in open-systems. These authors demonstrated that the ratio of alteration is significantly higher at all temperatures in open systems when compared to closed systems; this is caused by the change of solution, which accelerates the dissolution of the glass. If solutions are strongly alkaline, the addition of  $\text{Na}^+$  will favor the formation of zeolites. Removal of surplus alkalis triggers clay mineral precipitation (e.g., montmorillonite, as in the Cardiel Formation). Nevertheless, the abundance of montmorillonite in the Cardiel Formation is due either to the neof ormation from glass, or to infiltration. At this stage, zeolites are formed only as a by-pass, intermediate phase that disappear with increasing alteration degree (i.e., with increased removal of alkalis). This fact demonstrates the importance of permeability and percolation rates in natural systems.

Regarding the varieties of zeolites formed, Höller and Wirsching (1978) reported that the first zeolite formed in their experimental environment was phillipsite, a mineral phase that occurs in closed systems from silica-poor precursors. On the contrary, in open systems, the first zeolite formed was clinoptilolite, a silica-rich zeolite. With increasing alteration, the silica-rich zeolite mordenite was formed during the experiments. If alteration continues, the quantitative ratio of zeolites changes in favor of analcime, due to the continuous addition of  $\text{Na}^+$ . In general, this downward succession of authigenic minerals represents, as a whole, a decreasing hydration trend with depth (Irijima 1978).

In the case of the samples of the Cardiel Formation, only traces of probably mordenite were found in one sample (sample 12). Thus, the very scarce amount of mordenite (?) and analcime detected do not favor the hypothesis of the downward decreasing hydration rate, but supports the idea of a local increase in the  $\text{Na}^+/\text{K}^+$  ratio in the pore fluids (Ghiara *et al.* 2000) in order to allow the formation of mordenite (?). A slight increase in the pH of the interacting fluids would also have increased the  $\text{Na}^+/\text{K}^+$  ratio and decreased the Si/Al ratio, favoring the crystallization of analcime (Boles 1971). The early crystallization of smectite also supports the hypothesis of an open system, because smectite is generally absent in closed systems (Barth-Wirsching and Höller 1989).

Clinoptilolite-mordenite assemblage in open systems may be replaced by heulandite-analcime assemblages with depth in thick sequences of fresh water (or marine) deposits, as stated by Hay (1978). In the case of the Cardiel Formation, the clear predominance of clinoptilolite locates these deposits within the "A" diagenetic zone of Hay (1978) in open-hydrologic systems, corresponding to a non-analcime, alkali-rich zeolite zone.

## DEPOSITIONAL HISTORY

During the Cenomanian-middle Santonian, the northern portion of the Austral Basin was completely dominated by continental deposits (Nullo *et al.* 1999). The fast regres-

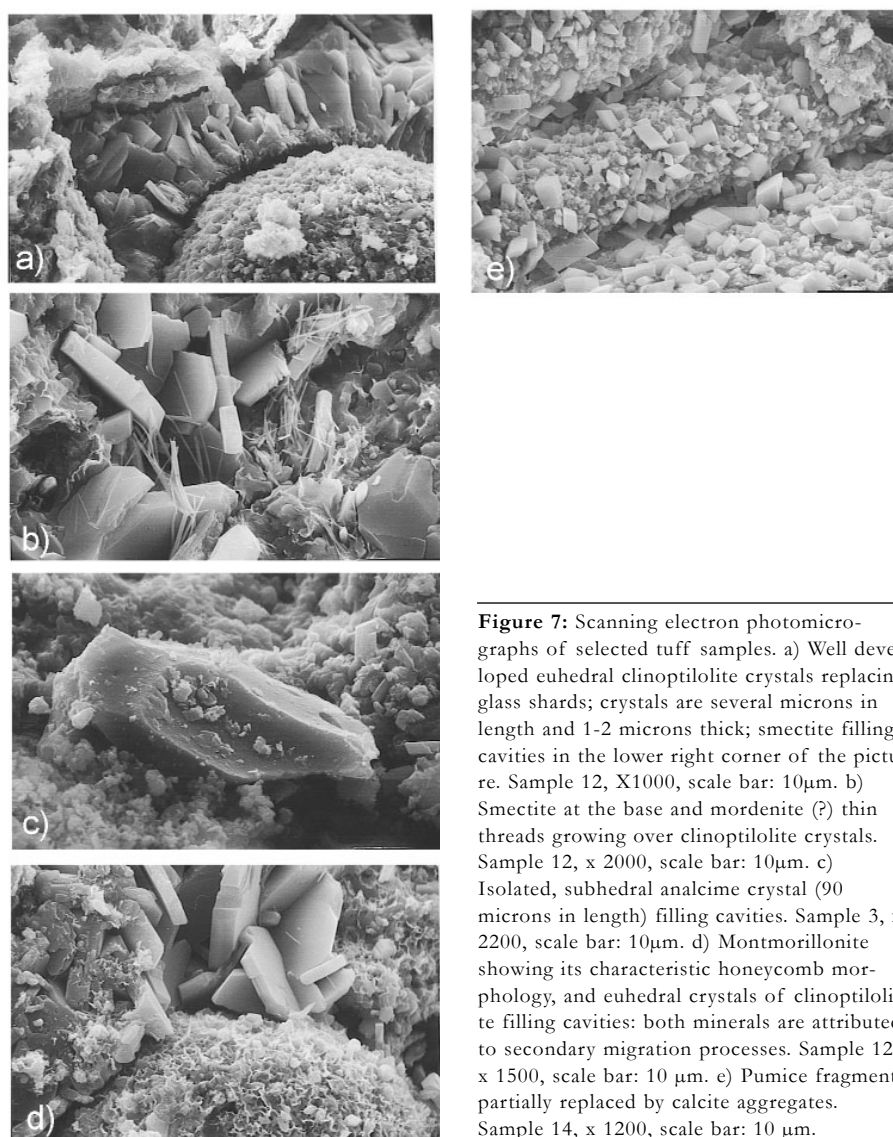


**Figure 7:** Scanning electron photomicrographs of selected tuff samples. a) Well developed euhedral clinoptilolite crystals replacing glass shards; crystals are several microns in length and 1-2 microns thick; smectite filling cavities in the lower right corner of the picture. Sample 12, X1000, scale bar: 10 $\mu\text{m}$ . b) Smectite at the base and mordenite (?) thin threads growing over clinoptilolite crystals. Sample 12, x 2000, scale bar: 10 $\mu\text{m}$ . c) Isolated, subhedral analcime crystal (90 microns in length) filling cavities. Sample 3, x 2200, scale bar: 10 $\mu\text{m}$ . d) Montmorillonite showing its characteristic honeycomb morphology, and euhedral crystals of clinoptilolite filling cavities: both minerals are attributed to secondary migration processes. Sample 12, x 1500, scale bar: 10  $\mu\text{m}$ . e) Pumice fragments partially replaced by calcite aggregates. Sample 14, x 1200, scale bar: 10  $\mu\text{m}$ .

sion of the sea during Albian times left extensive plains of very low relief exposed (Ramos 1982, Arbe 1989). The predominant sedimentary environment for the Cardiel Formation was thus represented by distal, flat alluvial plains associated with lagoons (Ramos 1982).

In the case analyzed in this work, fine-grained clastic sediments and volcanoclastic sandstones along with scarce tuffaceous sediments represent the base of the section (Fig. 2). Directional structures may appear included in thin lenticular channels, showing north- to northeast-, or less frequently, southwest-oriented paleocurrents. This orientation of the paleocurrents suggests the possibility of tidal currents in an environment of extended lagoons, where

some fine-grained carbonized vegetal debris and endichnia bioturbation may also appear. The existence of these tidal currents can also be supported by evidences of subaerial exposition such as the presence of thin reddish paleosols with axial roots and/or poorly developed prismatic structures (Fig. 2).

The occurrence of tuffs and bentonites abruptly increases towards the top of the section (Fig. 2) due to the deposition of pyroclastic-rich material on extended flat plains, thus covering the former lagoonal environment. Nevertheless, some epiclastic siltstones intercalated within the pyroclastic deposits suggest partial flooding of the plains due to sea level oscillations. Moreover, the presence of paleosols in tuffaceous

ous or bentonitic deposits with weak prismatic structure may also suggest sea level changes. In these plains, repeated ash-falls covered the paleosols previously developed on either tuffs or bentonites, reflecting changes in the sea level and brief episodes of air exposure.

Interpretation of the ash fall and volcanoclastic sandstones deposition

The volcanic arc located along the Patagonian Andes Mountains is associated to the magmatic activity related to the convergence of the Nazca and the Antarctic plates under the South American plate (Ramos 1999, Hervé *et al.* 2000, Ramos and Aguirre-Urreta 2000). As the ash-falls of the Cardiel Formation are registered at a distance of at least 100 km from the Andean chain, we interpret in this work an alternance of plinian and sub-plinian volcanism, and perhaps brief phreato-plinian processes (e.g., Cas and Wright 1987, Heiken and Wohletz 1992).

The plinian and sub-plinian volcanism is represented in the Cardiel Formation by highly vesicular pumices with small, slightly to highly elongated and even twisted vesicles, and also by shards that represent broken vesicle walls (plate, crescent, branched, and Y-shaped shards). The presence of few blocky massive shards with small vesicles to non-vesicular, together with pumices with low spherical and widely spaced vesicles, can be related to short phreato-plinian events (cf. Heiken and Wohletz 1992). The small amount of phenocrystals and cognate lithic clasts is remarkable in the plinian volcanism (cf. Heiken and Wohletz 1992). Lithic and even crystal-rich tuffites are largely of epiclastic origin (Cas and Wright 1987); these rocks are interpreted as being produced by the erosion and reworking of underlying tuffaceous deposits, and later deposited in shallow channels by tractive currents.

The origin of the glassy components of this unit is also related to the volcanoes located along the Andean chain, represented by composite cones and large calderas (cf. Heiken and Wohletz 1992). Volcanic-related processes covered the extra-Andean Patagonian plain with more than 1,500 m thick rhyolitic tuffs and their reworked products (tuffites) during the Cenomanian.

## CONCLUSIONS

The 196 m-thick section of the Cardiel Formation analyzed in this work includes several types of volcanoclastic sediments (79%), as well as claystones and siltstones (21%). Tuffs are classified as vitric or simple tuffs, whereas epiclastic tuffites include abundant lithic fragments, mostly tuffaceous and volcanic clasts. Paleosols were commonly developed, represented by the reddening on top of siltstones, tuff or bentonite deposits; in some cases, axial roots and poorly developed prismatic structures were also recognized.

The depositional history of the Cardiel Formation is related to a fast regression of the sea during Albian times, which left extensive low-relief plains exposed. Sedimentary environments interpreted at the base of the unit include distal alluvial plains and lagoons influenced by tidal currents. Occurrence of tuff and bentonites abruptly increases towards the top of the unit, due to the deposition of volcanic and volcanoclastic material on the extensive flat plains. Some epiclastic claystone and siltstone beds interbedded among the pyroclastic deposits may suggest the partial flooding of these plains. Moreover, the presence of the paleosols may also suggest sea level oscillations. Regarding the sequence of diagenetic events, textural evidences (such as the sequence of crystallization of the secondary mineral phases as revealed in thin section and under SEM) indicate that the order of crystallization of the diagenetic species was montmorillonite-zeolites-calcite-ferric oxides-hydroxides. Montmorillonite and zeolites are mainly related to the replacement of glass shards and pumice fragments. Tuffs and tuffites may show montmorillonite cutans due to an early migration and/or replacement process.

The first zeolite phase to crystallize as a replacement of the shards was clinoptilolite, identified by its Si/Al ratio. Clinoptilolite was in turn locally transformed into a more rare fibrous zeolite (modernite? erionite?) and very scarce analcime. This transformation could be attributed to a local increase in the Na<sup>+</sup>/K<sup>+</sup> ratio of the interacting fluids, which may have decreased the Si/Al ratio of the environment.

At a later stage, a very small-scale joint system, observed in thin sections, allowed a second migration phase of smectite along cracks and enlarged secondary vugs, followed by the precipitation of big zeolite crystals (in geodes) and late calcite. Some analcime that precipitated in fissures may also be related to this late migration process. Several shards and pumices were replaced by calcite. The latest diagenetic process is represented by the migration of iron oxides and hydroxides associated to the replacement of glass shards, causing the staining of almost all shards (tuffs) and even zeolites previously precipitated in secondary vugs. From field evidence and paragenesis, we conclude in this work that the origin of zeolites minerals in the Cardiel Formation can be assigned to percolating waters in an open-hydrologic system. The clear predominance of clinoptilolite situates these deposits into the "A" diagenetic zone of Hay (1978), in an open-hydrologic system, where it coexists with smectite.

## WORKS CITED IN THE TEXT

- Arbe, H. A. 1989. Estratigrafía, discontinuidades y evolución sedimentaria del Cretácico en la Cuenca Austral, provincia de Santa Cruz. In Cuenas Sedimentarias Argentinas, Chebli, G.A. and Spalletti, L.A. (eds.) Universidad Nacional de Tucumán, Instituto Superior de Correlación Geológica 419-442, Tucumán.
- Barth-Wirsching, U. and Höller, H. 1989. Experimental studies on zeolite formation conditions. *European Journal Mineralogy* 1: 489-506.
- Boles, J.R. 1971. Synthesis of analcime from natural heulandite and clinoptilolite. *Annals Mineralogy* 56: 1724-1734.
- Brewer, R. 1964. Fabric and mineral analysis of soils. J. Wiley and Sons, 470 p., New York.
- Bullock, P., Fedoroff, N., Jongerius, A., Stoops, G. and Tursina, T. 1985. Handbook for soil thin section description. Waine Research Publ., 152 p., United Kingdom.
- Cas, R.A.F. and Wright, J.V. 1987. Volcanic successions. *Modern and Ancient*. Allen and Unwin, 528 p., London.
- Coombs, D.S. and Whetten, J.T. 1967. Composition of analcime from sedimentary and burial metamorphic rocks. *Geological Society of America Bulletin* 78: 269-282.

- Folk, R. L., Andrews, P. B., and Lewis, D. W. 1970. Detrital sedimentary rock classification and nomenclature for use in New Zealand. *New Zealand Journal of Geology and Geophysics*, 13: 937-968.
- Fossa Mancini, E., Feruglio, E. and Yussen de Campana, J.C. 1938. Una reunión de geólogos de YPF y el problema de la terminología estratigráfica. *Boletín Informaciones Petroleras* 171: 31-95, Buenos Aires.
- Ghiara, M.R., Petti, C., Franco, E. and Lonis, R. 2000. Distribution and genesis of zeolites in Tertiary ignimbrites from Sardinia: evidence of superimposed mineralogenic processes. In Colella, C. and Mumpton, F.A. (eds.) *Natural Zeolites for the Third Millennium*. De Frere Editore, 177-192, Napoli.
- Greene-Kelley, R. 1953. The identification of montmorillonite in clays. *Journal Soil Science* 4: 233-237.
- Hay, R.L. 1978. Geologic occurrence of zeolites. In Sand, L.B. and Mumpton, F.A. (eds.) *Natural Zeolites. Occurrence, Properties, Use*. Pergamon Press, 135-143.
- Heiken, G. and Wohletz, K., 1992. *Volcanic Ash*. University of California Press, 2d. printing, 246 p., Berkeley.
- Hervé, F., Demant, A., Ramos, V.A., Pankhurst, R. and Suarez, M. 2000. The Southern Andes. In Cordani, U.G., Milani, F., Thomaz Filho, A. and Campos, D.A. (eds.), *Tectonic evolution of South America*, 31st International Geological Congress, 605-634, Rio de Janeiro.
- Höller, H. and Wirsching, U. 1978. Experiments on the formation of zeolites by hydrothermal alteration of volcanic glasses. In Sand, L.B. and Mumpton, F.A. (eds.) *Natural Zeolites. Occurrence, Properties, Use*, Pergamon Press, 329-336.
- Irijima, A. 1978. Geological occurrences of zeolite in marine environments. In Sand, L.B. and Mumpton, F.A. (eds.) *Natural Zeolites. Occurrence, Properties, Use*, Pergamon Press, 175-198.
- Mazzoni, M. M. 1986. Procesos y depósitos piroclásticos. *Asociación Geológica Argentina, Serie B, Didáctica y Complementaria* 14, 115 p., Buenos Aires.
- Nullo, F.E., Panza, J. L. and Blasco, G. 1999. El Jurásico y Cretácico de la Cuenca Austral. In Caminos, R. (ed.) *Geología Argentina*, 528-535, Buenos Aires.
- Pettijohn, F.J., Potter, P.E., and Siever, R. 1987. *Sand and Sandstone (Second Edition)*. Springer-Verlag, 553 p., New York.
- Piatnizky, A. 1938. Observaciones geológicas en el oeste de Santa Cruz (Patagonia). *Boletín Informaciones Petroleras* 165: 45-85, Buenos Aires.
- Pöthe de Baldis, D. 1978. Estudio palinológico de muestras correspondientes a distintas formaciones y localidades de las Hojas 55 a y b, Provincia de Santa Cruz. Servicio Geológico Nacional (unpublished) Buenos Aires.
- Ramos, V.A. 1982. Geología de la región del lago Cardiel, provincia de Santa Cruz. *Asociación Geológica Argentina, Revista*, 37(1): 23-49, Buenos Aires.
- Ramos, V.A. 1999. Plate tectonic setting of the Andean Cordillera. *Episodes* 22(3): 183-190.
- Ramos, V.A. and Aguirre-Urreta, M.B. 2000. Patagonia. In Cordani, U.G., Milani, F., Thomaz Filho, A. and Campos, D.A. (eds.), *Tectonic evolution of South America*, 31st International Geological Congress, 369-380, Rio de Janeiro.
- Rodríguez-Carvajal, J. 1990. FULLPROF: A program for Rietveld refinement and pattern matching analysis. In: *Satellite Meeting on Powder Diffraction of the XV Congress of the International Union Crystallography. Abstracts*, 127, Toulouse, France.
- Ruiz, L.G. 1984. Plantas fósiles cretácicas procedentes de la zona del lago Cardiel, provincia de Santa Cruz. IX° Congreso Geológico Argentino, Actas 4: 444-454, Bariloche.
- Russo, A. and Flores, M.A. 1972. Patagonia Austral extraandina. In Leanza, A.P. (ed.) *Geología Regional Argentina*, Academia Nacional de Ciencias, 1: 707-725, Córdoba.
- Russo, A., Flores, M.A. and Di Benedetto, H. 1978. Patagonia Austral extraandina. In Turner, J.C. (ed.), *Geología Regional Argentina*. Academia Nacional de Ciencias, 2: 1431-1462, Córdoba.
- Saha, P. 1959. Geochemical and X-ray investigation of natural and synthetic analcites. *American Mineralogist* 44: 300-313.
- Teruggi, M. E., Mazzoni, M. M., Spalletti, L. A. and Andreis, R. R. 1978. Rocas piroclásticas. Interpretación y Sistemática. *Asociación Geológica Argentina, Publicaciones Especiales, Serie B (Didáctica y Complementaria)* 5, 36 p., Buenos Aires.
- Young, R. A. 1993. *The Rietveld Method*. International Union Crystallography, Oxford University Press, 298 p., New York.
- Ugarte, F.R.E. 1956. Relevamiento geológico expeditivo de la zona del lago Cardiel. Yacimientos Carboníferos Fiscales, Buenos Aires (unpublished).
- Wilkinson, J.F.G. and Whetten, J.T. 1964. Some analcime-bearing pyroclastic and sedimentary rocks from New South Wales. *Journal of Sedimentary Petrology* 34: 543-553.

Recibido: 20 de abril, 2006

Aceptado: 27 de diciembre, 2006